Equations of Motion of a Quasisteady Flight Vehicle Utilizing Restrained Static Aeroelastic Characteristics

William P. Rodden* and J. Richard Love†
Northrop Corporation, Pico Rivera, California

Mean axes provide the usual reference in maneuvering and dynamic response analyses of flexible vehicles. Attached or structural axes have also been used because the flexibility characteristics of the structure are only determined for a restrained structure. If the structural axes are employed, a relationship is required for the orientations of the structural axes relative to the mean axes, since the equations of motion determine the orientations of the mean axes. If this relationship is not considered, as it has not been in a number of publications, the solution to the equations of motion of the structural axes is *not invariant* with the choice of support configuration used in the calculation of the structural flexibility influence coefficients and is, therefore, incorrect. This relationship and the correct equations of motion for the structural axes are presented, and the correctness of the formulation is demonstrated numerically in studies of longitudinal maneuvering of an example forward-swept-wing airplane at constant forward velocity. Although the paper assumes constant airspeed in the basic developments, it concludes with discussions of aeroelastic speed derivatives and aeroelastic effects on drag. The paper assumes quasisteady equilibrium of the structure with its applied loads throughout.

Nomenclature

A = aeroelastic deflection amplification factor
a = flexibility, a_F is free-body flexibility
a_s = amplitude of motion of support reference point
a_0 = airfoil two-dimensional lift curve slope
B = aeroelastic load amplification factor
b = reference span
C = generalized aerodynamic force coefficient: C_i is inertial value, C_q is angular rate value, C_α is incidence and control surface value, $C_{\dot\alpha}$ is incidence rate value, C_0 is initial value
C_e = experimental control point force coefficient
$\bar{C}_h$ = complex oscillatory aerodynamic influence coefficient
C_{hs} = static aerodynamic influence coefficient
C_m = aerodynamic pitching moment coefficient
C_z = aerodynamic normal force coefficient
$\bar{c}$ = mean aerodynamic chord
c_{l_α} = local lift curve slope
EI_x = bending stiffness
F = control point force: F_a is aerodynamic force, F_i is inertial force
GJ = torsional stiffness
g = acceleration of gravity; structural damping coefficient
H = generalized reference deflection: H_q includes steady angular rates, H_α includes changes in incidence and control surface rotations, $H_{\dot\alpha}$ includes incidence rates
h = control point deflection: h_f is flexible deformation, h_m is relative to mean axis, h_R is due to rigid body modes, h_r is due to rigid displacements, h_0 is initial value
I = unit matrix
I_y = pitching moment of inertia about support reference point
i_t = horizontal tail setting
k = reduced frequency
M = mass; Mach number
$\mathfrak{M}$ = generalized rigid body mass
n_z = normal load factor
q = pitch rate
$\bar{q}$ = dynamic pressure
R = inertial relief factor
$R\ell$ = real part of complex variable
S = reference surface area
S_y = static unbalance about support reference point
t = time
V = velocity
v = perturbation velocity
$\bar{x}$ = distance from support origin to center of gravity, positive forward
z_s = deflection of origin of structural support, positive downward
α = incidence (angle of attack): α_m is incidence of mean axis, α_s is incidence of structural axis
$\dot\alpha$ = incidence rate defined in Eq. (38)
β = sideslip angle
ΔC_α = supplementary incidence coefficient
ΔC_q = supplementary rate coefficient
δ = control surface rotation
θ = pitch angle of mean axis
λ = planform sweep angle

Subscripts and Superscripts

α = $\partial/\partial\alpha$
$\dot\alpha$ = $\partial/\partial(\dot\alpha\bar{c}/2V)$
q = $\partial/\partial(\dot\theta\bar{c}/2V)$
$\ddot{z}$ = $\partial/\partial(\ddot{z}_s/g)$
$\ddot\theta$ = $\partial/\partial(\ddot\theta\bar{c}/2g)$
v = $\partial/\partial(v/V)$
0 = intercept value at zero incidence
$\dot{(\ )}$ = $d(\ )/dt$
$\ddot{(\ )}$ = $d^2(\ )/dt^2$
$(\ )''$ = denotes FLEXSTAB value

Presented as Paper 84-0986 at the AIAA/ASME/ASCE/AHS 25th Structures, Structural Dynamics and Materials Conference, Palm Springs, CA, May 14-16, 1984; received June 4, 1984; revision received March 12, 1985.

*Consultant. Fellow AIAA
†Senior Technical Specialist, Dynamics and Loads, Advanced Systems Division.

Matrices

[ ] = square
$[\ ]^T$ = transpose
$[\ ]^{-1}$ = inverse
{ } = column

Introduction

THE use of a mean axis system as a reference for the equations of motion has been a standard in vibration and flutter analysis of unrestrained vehicles for many years. In 1962 a comprehensive statement of the various structural dynamics problems of the unrestrained vehicle was given by Bisplinghoff and Ashley[1] using a centroidal mean axis system. The use of attached, mean, and principal axes was discussed by Milne in 1964[2] and the distinction between mean and principal axes was further clarified in 1968.[3] The mean and principal axes are the same when transverse displacement is the primary degree of freedom, i.e., when rotatory inertia effects can be neglected (as we assume in the present development). The use of a mean axis system in flight mechanics was further refined in the FLEXSTAB computer program developed by Dusto and his associates at the Boeing Co. from 1968[4] to 1974.[5] The conclusion from those investigations was that mean axes, rather than attached axes, must be used in the equations of motion.

In 1965 Wykes and Lawrence[6] utilized both mean and attached axes in a study of aerothermoelastic effects on the stability and control of a typical canard-delta configuration. Their "modal technique" used the mean axes and their "direct influence coefficient technique" used the attached axes. Wykes and Lawrence recognized both the need for the mean axes and the difficulties associated with the attached axes: "The main problem stems from the fact that it is very difficult to obtain readily a transformation relating the angle-of-attack reference used in the influence coefficient problem analyses to the angle-of-attack reference of the dynamic stability problem formulation. In the influence coefficient analyses, the angle-of-attack reference was a line tangent to the wing surface slope at the wing apex. This was a convenient choice, for it permitted the most expedient joining of vehicle component effects to form the whole. In the dynamic stability analyses, the reference line for angle of attack was a body axis related to mass characteristics and rigid vehicle main lifting surface orientation. This axes system was the one for which the equations of motion were written. It is pertinent also to emphasize that this axes system is the same one used for the modal analyses described earlier. For this reason, the difficulty being discussed is avoided in the modal technique and constitutes another advantage in its application in connection with most dynamic aerothermoelastic problems. Although one does know the orientation of the velocity vector (and, consequently, the angle of attack) with respect to the reference system attached at the wing apex, the relationship difficult to define is the angle between the flexible vehicle wing apex axes and the equations of motion axes."

In spite of all the foregoing developments, two textbooks and one NASA report have appeared subsequently that prefer the convenience of the attached axes without regard to the requirements for the mean axes. In his two books on airplane flight dynamics, where Roskam[7,8] addresses stability and control of the elastic airplane, he chooses the origin of the attached axis system at "a reference point in the jig shape" which "is also the material point that represents the center of gravity (c.g.) of the jig shape." The facts that there may be no structural connection to the c.g., and that the c.g. does not remain fixed during a mission, are not addressed. Then, Kemp[9] chooses the origin of his attached axis system at 33% of the mean aerodynamic chord because the structural influence coefficients (SIC's) used in a Boeing study of a high-performance supersonic transport airplane configuration were fixed there. However, he notes that "when a complete and consistent set of stability derivatives is used in the equations of motion derived from the conditions for dynamic equilibrium, the reactions at the fixity point vanish and the deformed shape at any instant is, in a coordinate-free sense, independent of fixity point location."

References 7-9 have one assumption in common: that the solution to the equations of motion will be invariant with the choice of support system used to determine the SIC's if this support system is unloaded in the unrestrained flight condition. This is a necessary and sufficient condition for a trimmed loads solution only, and the loads solution of Rowan and Burns[10] is, therefore, correct. However, it is not sufficient for the maneuvering solution. The conditions for a correct maneuvering solution require not only an unloaded support system but also, and obviously, that the moment equals the rate of change of angular momentum. These conditions will be realized if the mean axis formulation of the equations of motion is employed. However, an alternative formulation that retains the convenience of an arbitrary attached axis system can still be used if the location of the mean axes is duly noted in the formulation. This alternative formulation is the subject of the present paper.

The attached axes will be called structural axes in this paper because they will be referred to the statically determinate support system for which the SIC's are determined, and, in general, the assumption of constant forward velocity will be made here, although the problem of calculating speed derivatives for lift and moment by numerical differentiation of the present results will be discussed briefly.

Aeroelastic Characteristics of a Restrained Vehicle

For the analysis of the aeroelastic characteristics of a restrained vehicle the vehicle flexibility can be represented by a matrix of SIC's which permits the calculation of the structural deflections relative to a statically determinate support system [the SIC constraint points(s)] located conveniently within the vehicle (e.g., near the intersection of primary wing and fuselage structural components). The aeroelastic analysis must consider not only the aerodynamic forces that arise from vehicle incidence and control surface rotations but also the aerodynamic forces that arise from the deflections (considered as initial deflections such as camber and twist) caused by the inertial forces that would exist in free flight. This approach leads to a series of inertial aeroelastic coefficients corresponding to unit dimensionless accelerations in addition to the more conventional aeroelastic coefficients. An example of this approach is given in Sec. 8-3 of Ref. 11, in which the effect of normal load factor on a wing is considered.

The net force distribution $\{F\}$ acting on a flexible lifting surface or body is the difference between the aerodynamic forces $\{F_a\}$ and the inertial forces $\{F_i\}$,

$$\{F\} = \{F_a\} - \{F_i\} \tag{1}$$

The aerodynamic forces are found from experimentally corrected,‡ steady aerodynamic influence coefficients (AIC's) $[C_{hs}]$ defined in Ref. 12, and a set of experimentally determined control force coefficients $\{C_e\}$.

$$\{F_a\} = (\bar{q}S/\bar{c}\,)[C_{hs}]\{h\} + \bar{q}S\{C_e\} \tag{2}$$

The use of the experimental force coefficients may be necessary to account for aerodynamic effects that are not predictable, such as some interference loads, or not accurately predictable, such as camber loads. The inertial forces are

‡A premultiplying correction matrix derived from experimental data on loads arising from vehicle rotations of incidence and control surfaces is discussed in Refs. 12 and 13. Reference 13 also considers a postmultiplying correction matrix.

found from the mass matrix $[M]$ and the accelerations

$$\{F_i\} = [M]\{\ddot{h}\} \tag{3}$$

The accelerations are written in terms of the rigid body modal matrix $[h_R]$ of Ref. 14 and the accelerations of a reference point in the SIC support system, and by neglecting any dynamic structural response

$$\{\ddot{h}\} = [h_R]\{\ddot{a}_s\} \tag{4}$$

The accelerations $\{\ddot{a}_s\}$ are assumed to be known.

The deflections $\{h\}$ are given by the sum of the deflections of the rigid vehicle $\{h_r\}$[§] and the flexible deflections $\{h_f\}$ relative to the support system.

$$\{h\} = \{h_r\} + \{h_f\} \tag{5}$$

The last equation required for the aeroelastic analysis is the flexibility relationship. The flexible deflections are found from the SIC's $[a]$ and the net forces.

$$\{h_f\} = [a]\{F\} \tag{6}$$

Substituting Eqs. (1-5) into Eq. (6) permits solution for the flexible deflections

$$\{h_f\} = [A][a]\{F_r\} \tag{7}$$

where $\{F_r\}$ is the net force distribution on the rigid vehicle

$$\{F_r\} = (\bar{q}S/\bar{c})[C_{hs}]\{h_r\} + \bar{q}S\{C_e\} - [M][h_R]\{\ddot{a}_s\} \tag{8}$$

and $[A]$ is the aeroelastic deflection amplification (or attenuation) matrix

$$[A] = ([I] - (\bar{q}S/\bar{c})[a][C_{hs}])^{-1} \tag{9}$$

The net force distribution on the flexible vehicle is obtained by substituting Eqs. (2-8) into Eq. (1)

$$\{F\} = [B]\{F_r\} \tag{10}$$

where $[B]$ is the aeroelastic load amplification (or attenuation) matrix

$$[B] = [I] + (\bar{q}S/\bar{c})[C_{hs}][A][a] \tag{11a}$$

$$= ([I] - (\bar{q}S/\bar{c})[C_{hs}][a])^{-1} \tag{11b}$$

The alternative form for $[B]$ shown in Eq. (11b) would have been obtained if the order of solution for $\{h_f\}$ and $\{F\}$ above had been reversed. The use of Eq. (11a) is more computationally efficient since a second matrix inversion is not required. A singularity in $[A]$ (and $[B]$) occurs at the eigenvalues of

$$(\bar{c}/S\bar{q})\{h_f\} = [a][C_{hs}]\{h_f\} \tag{12}$$

(Note that Eqs. (9) and (11b) have identical singularities.) Aeroelastic divergence of the *restrained vehicle* corresponds to positive values of $\bar{c}/S\bar{q}$.

The analysis of equilibrium and the determination of stability derivatives requires the generalization of the initial deflections $\{h_r\}$ introduced above. It is written

$$\{h_r\} = \{h_0\} + [h/H_\alpha]\{H_\alpha\} + [h/H_q]\{H_q\} \tag{13}$$

§These deflections arise from a number of sources: built-in twist, camber, or thermal distortions; changes in incidence or control surface rotations; steady angular motions. A number of terms to account for these effects separately are introduced in Eq. (13).

The first term $\{h_0\}$ accounts for initial deflections such as camber and twist, and thermoelastic deflections which may be important in flight at high supersonic speeds at low altitudes. The second term accounts for changes in incidence and control surface deflections; e.g., if in the longitudinal case the elements of $\{H_\alpha\}$ are angle of attack and elevator rotation, then the elements of the first column of $[h/H_\alpha]$ are streamwise distances of the aerodynamic control points from the pitch axis, and the second column consists of non-zero elements on the control surface equal to the streamwise distances from the hinge line. The third term in Eq. (13) accounts for steady angular velocities, such as pitch rate or roll rate; e.g., if one element of $\{H_q\}$ is pitch rate, the elements in the corresponding column of $[h/H_q]$ are proportional to the square of the streamwise distances of the aerodynamic control points from the pitch axis.[15]

The rigid body modal matrix $[h_R]$ also provides the basis for the equilibrium condition, viz., that there are no net resultant forces in any direction or resultant moments about any axis, i.e.,

$$[h_R]^T\{F\} = 0 \tag{14}$$

Substituting Eqs. (8), (10), and (13) into Eq. (14) leads to the basic equilibrium equation which can be written

$$\bar{q}S(\{C_0\} + [C_\alpha]\{H_\alpha\} + [C_q]\{H_q\} + [C_i]\{\ddot{a}_s\}) - [\mathfrak{M}]\{\ddot{a}_s\} = 0 \tag{15}$$

where the initial coefficient matrix is

$$\{C_0\} = [h_R]^T[B]((1/\bar{c})[C_{hs}]\{h_0\} + \{C_e\}) \tag{16}$$

the incidence coefficient matrix is

$$[C_\alpha] = (1/\bar{c})[h_R]^T[B][C_{hs}][h/H_\alpha] + [\Delta C_\alpha] \tag{17}$$

and the angular rate coefficient matrix is

$$[C_q] = (1/\bar{c})[h_R]^T[B][C_{hs}][h/H_q] + [\Delta C_q] \tag{18}$$

We have introduced a supplementary incidence coefficient matrix $[\Delta C_\alpha]$ and a supplementary rate coefficient matrix $[\Delta C_q]$ above because there are certain theoretical difficulties in estimating lateral-directional stability derivatives from AIC's (e.g., the wing rotary cross-derivatives and the adverse yawing moment from ailerons). These supplementary matrices must be obtained from other considerations than those presented here. The aerodynamic loads induced by inertial forces have been separated from the rigid body inertial forces so the inertial coefficient matrix is given by

$$\bar{q}S[C_i] = [h_R]^T([I] - [B])[M][h_R] \tag{19a}$$

$$= -(\bar{q}S/\bar{c})[h_R]^T[C_{hs}][A][a][M][h_R] \tag{19b}$$

and the rigid body inertial matrix is

$$[\mathfrak{M}] = [h_R]^T[M][h_R] \tag{20}$$

Unsteady aerodynamic effects, contained in $\dot{\alpha}$- and $\dot{\beta}$-derivatives, have not yet been considered in the present development. They may be obtained by using complex AIC's $[\bar{C}_h]$, defined in a similar manner to $[C_{hs}]$, and utilizing the method of Ref. 15. Accordingly, Eq. (15) will be extended to include these effects by adding the term $[C_{\dot{\alpha}}]\{H_{\dot{\alpha}}\}$. The method of Ref. 15 leads to the rigid $\dot{\alpha}$- and $\dot{\beta}$- loadings which, when introduced into the foregoing development, result in the expression

$$[C_{\dot{\alpha}}] = -R\ell(1/2k^2)[h_R]^T[B][\bar{C}_h][h/H_{\dot{\alpha}}] \tag{21}$$

where k is the reduced frequency based on some characteristic frequency of the vehicle, e.g., the short period mode or Dutch roll mode, for which the oscillatory AIC's are obtained, and the columns of $[h/H_{\dot{\alpha}}]$ are the displacements for unit plunging for $\dot{\alpha}$ and unit sidesway for $\dot{\beta}$. The extended form of Eq. (15) then appears as

$$\bar{q}S(\{C_0\}+[C_\alpha]\{H_\alpha\}+[C_{\dot{\alpha}}]\{H_{\dot{\alpha}}\}+[C_q]\{H_q\} + [C_i]\{\ddot{a}_s\})-[\mathfrak{M}]\{\ddot{a}_s\}=0 \tag{22}$$

The stability derivative data are all contained in the coefficient matrices in Eq. (22). Some of the terms in these coefficient matrices are dimensional and obtaining dimensionless aerodynamic coefficients from them depends on the rigid body motions considered. Different reference lengths are used to nondimensionalize the longitudinal coefficients from what are used for the lateral-directional coefficients, viz., the reference chord $\bar{c}$ in the longitudinal case and the reference span b in the lateral-directional case. In the longitudinal case, the trim parameters are angle of attack α_s and elevator deflection δ so

$$\{H_\alpha\}=\begin{Bmatrix}\alpha_s\\ \delta\end{Bmatrix} \tag{23}$$

and the rigid body degrees of freedom are plunge and pitch so that

$$[C_\alpha]=\begin{bmatrix}C_{z_\alpha} & C_{z_\delta}\\ C_{m_\alpha}\bar{c} & C_{m_\delta}\bar{c}\end{bmatrix} \tag{24}$$

Just as the incidence and control effectiveness derivatives are found from $[C_\alpha]$, in a similar manner the initial aerodynamic derivatives can be found from $\{C_0\}$ and the aerodynamic damping derivatives can be found from $[C_{\dot{\alpha}}]$ and $[C_q]$. Finally, the aerodynamic inertial derivatives are found from $[C_i]$. In the longitudinal case

$$\{\ddot{a}_s\}=\begin{Bmatrix}\ddot{z}_s\\ \ddot{\theta}\end{Bmatrix} \tag{25}$$

and if we define dimensionless inertial derivatives by

$$C_z=C_{z_{\ddot{z}}}(\ddot{z}_s/g)+C_{z_{\ddot{\theta}}}(\ddot{\theta}\bar{c}/2g) \tag{26}$$

and

$$C_m=C_{m_{\ddot{z}}}(\ddot{z}_s/g)+C_{m_{\ddot{\theta}}}(\ddot{\theta}\bar{c}/2g) \tag{27}$$

we find

$$[C_i]=\begin{bmatrix}C_{z_{\ddot{z}}} & C_{z_{\ddot{\theta}}}\bar{c}\\ C_{m_{\ddot{z}}}\bar{c} & C_{m_{\ddot{\theta}}}\bar{c}^2\end{bmatrix} \tag{28}$$

The FLEXSTAB Formulation for the Unrestrained Vehicle

It can be inferred from the FLEXSTAB documents,[4,5] that the foregoing development for the restrained vehicle also applies to the unrestrained vehicle if the free-body flexibility matrix $[a_F]$ replaces the restrained SIC's where

$$[a_F]=[R][a][R]^T \tag{29}$$

and [R] is the inertial relief matrix

$$[R]=[I]-[h_R][\mathfrak{M}]^{-1}[h_R]^T[M] \tag{30}$$

Substituting Eq. (29) into Eqs. (9), (11), and (16-18) leads to aerodynamic coefficients for the unrestrained vehicle; the inertial coefficients, Eq. (19), do not exist in the FLEXSTAB formulation because all inertial relief effects have been accounted for in the free-body SIC's. Equation (22) (with the term $[C_i]\{\ddot{a}_s\}$ deleted) becomes the equation of motion and $\{\ddot{a}_s\}$ is the set of accelerations of a point on the mean axis *at the longitudinal location of the origin of the support system,* and it then appears as

$$\bar{q}S(\{C_0''\}+[C_\alpha'']\{H_\alpha''\}+[C_{\dot{\alpha}}'']\{H_{\dot{\alpha}}''\} + [C_q'']\{H_q''\})-[\mathfrak{M}]\{\ddot{a}_s\}=0 \tag{31}$$

where the doubly primed coefficients are the FLEXSTAB values (see Ref. 16 for an alternative derivation of the FLEXSTAB coefficients beginning with the restrained values of the preceding section).

Maneuvering of an Unrestrained Vehicle

Equation (31) is the correct equation of motion for the quasisteady maneuvering vehicle. However, Eq. (22) was implicitly assumed to be valid in Refs. 7-9, but, as noted in the Introduction, it contains no reference to the mean axis. The problem has been succinctly summarized by Letsinger: "If angular accelerations are not measured with respect to the mean plane,...equations 1 and 2 [Eq. (22) here] will not be valid. The motion of the axes system will not represent the motion of the airplane. Figure 2 [Fig. 1 here] illustrates the problem. Three possible clamp locations are shown. A 'clamped axis' is shown at each clamp point. If the load on the airplane is changing, the airplane shape is also changing. If the airplane shape is changing, the three clamped axes are rotating relative to each other. Therefore, no more than one of the axes shown can possibly have a pitch acceleration time history proportional to the pitching moment time history. Or, at any given instant, no more than one clamped axis can have a pitch rate proportional to the angular momentum of the system. In general, the clamped axes system does not relate to the equations of motion."[17]

Accordingly, the accelerations $\{\ddot{a}_s\}$ in Eq. (22) are interpreted to be the accelerations of Eq. (31), i.e., *of a point on the mean axis at the support station.* Then, since the equations of motion now contain the angle of attack at the support and the rotation angle of the mean axis, a relationship is needed between the angles; this is the relationship that Wykes and Lawrence[6] did not obtain (see Introduction). Figure 2 illustrates the geometry.

The deflections of the structure relative to the mean axes $\{h_m\}$ may be written

$$\{h_m\}=\{h_f\}+[h_R]\{a_s\} \tag{32}$$

in which $\{a_s\}$ now represents the set of displacements (translations and rotations) of the support point relative to the mean axes. The requirement for the mean axes is that deformation occurs about them such that the center of gravity does not move and the axes do not rotate.[2,3] In terms of the rigid-body modal matrix and the mass matrix, this condition is expressed by

$$[h_R]^T[M]\{h_m\}=0 \tag{33}$$

Equations (32) and (33) lead to

$$\{a_s\}=-[\mathfrak{M}]^{-1}[h_R]^T[M]\{h_f\} \tag{34}$$

The rotations of the structural axes relative to the mean axes are given by certain elements of $\{a_s\}$. If the deflections $\{h_f\}$ are calculated independently for each source of loading, viz., initial deflections, incidence and control surface deflections, angular rates, and accelerations of the support point, via Eq. (7) for the restrained vehicle, then the values of the appropriate rotational elements in $\{a_s\}$, properly adjusted in sign, can be used as coefficients in the following equation for the angles of attack (longitudinal and sideslip) of the longitudinal mean axis.

$$\{\alpha_m\} = \{\alpha_{m_0}\} + [\partial\alpha_m/\partial\alpha]\{H_\alpha\} + [\partial\alpha_m/\partial\dot{\alpha}]\{H_{\dot{\alpha}}\} + [\partial\alpha_m/\partial q]\{H_q\} + [\partial\alpha_m/\partial\ddot{a}]\{\ddot{a}_s\} \quad (35)$$

It will be demonstrated by numerical calculations that Eq. (22) coupled with Eq. (35) is equivalent to Eq. (31). An example airplane in a typical pitch maneuver will be investigated using three significantly different support configurations and the solutions will be compared to the FLEXSTAB solution.

The Quasisteady Longitudinal Equations of Motion

We now rewrite Eqs. (22) and (35) for the case of longitudinal motion so that specific details in their solution will become apparent. Equation (22) is expanded to read

$$\bar{q}S\left(\begin{Bmatrix} C_{z_0} \\ C_{m_0}\bar{c}\end{Bmatrix} + \begin{bmatrix} C_{z_\alpha} & C_{z_\delta} \\ C_{m_\alpha}\bar{c} & C_{m_\delta}\bar{c}\end{bmatrix}\begin{Bmatrix}\alpha_s \\ \delta\end{Bmatrix} + \begin{bmatrix} C_{z_{\dot{\alpha}}} & C_{z_q} \\ C_{m_{\dot{\alpha}}}\bar{c} & C_{m_q}\bar{c}\end{bmatrix} \times \begin{Bmatrix}\dot{\alpha}\bar{c}/2V \\ \dot{\theta}\bar{c}/2V\end{Bmatrix} + \begin{bmatrix} C_{z_{\ddot{z}}} & C_{z_{\ddot{\theta}}} \\ C_{m_{\ddot{z}}}\bar{c} & C_{m_{\ddot{\theta}}}\bar{c}\end{bmatrix}\begin{Bmatrix}\ddot{z}_s/g \\ \ddot{\theta}\bar{c}/2g\end{Bmatrix}\right) - \begin{bmatrix} M & S_y \\ S_y & I_y\end{bmatrix}\begin{Bmatrix}\ddot{z}_s \\ \ddot{\theta}\end{Bmatrix} = 0 \quad (36)$$

Equation (35) becomes

$$\alpha_m = \alpha_{m_0} + \alpha_{m_\alpha}\alpha_s + \alpha_{m_\delta}\delta + \alpha_{m_{\dot{\alpha}}}\dot{\alpha}\bar{c}/2V + \alpha_{m_q}\dot{\theta}\bar{c}/2V + \alpha_{m_{\ddot{z}}}\ddot{z}_s/g + \alpha_{m_{\ddot{\theta}}}\ddot{\theta}\bar{c}/2V \quad (37)$$

The rate of change of angle of attack is proportional to the centripetal acceleration of the vehicle, and is given by

$$\dot{\alpha} = (\ddot{z}_s - \bar{x}\ddot{\theta} + V\dot{\theta} + g\cos\theta)/V \quad (38)$$

where $\bar{x}$ is the distance from the origin of the support to the center of gravity. Since $\dot{\alpha}$ arises from plunging of the vehicle,[15] it must be invariant with the choice of structural axis, and using the centroidal acceleration in Eq. (38) leads to that invariance. That Eq. (38) is correct is also demonstrated in the study of the different structural axes in the example maneuver below.

The solution of Eqs. (36) and (37) requires their combination into a single matrix differential equation that results from the elimination of α_s. Substituting Eq. (38) into Eq. (37) and solving for α_s yields

$$\alpha_s = (1/\alpha_{m_\alpha})[\alpha_m - \alpha_{m_0} - (\alpha_{m_q} + \alpha_{m_{\dot{\alpha}}})\dot{\theta}\bar{c}/2V - (2\alpha_{m_{\ddot{z}}}V^2 + \alpha_{m_{\dot{\alpha}}}\bar{c}g)\ddot{z}_s/2gV^2 - (\alpha_{m_{\ddot{\theta}}}V^2 - \alpha_{m_{\dot{\alpha}}}\bar{x}g)\ddot{\theta}\bar{c}/2gV^2 - \alpha_{m_{\dot{\alpha}}}\bar{c}g\cos\theta/2V^2] \quad (39)$$

Substituting Eqs. (38) and (39) into Eq. (37) eliminates α_s and the equations of motion become

$$\begin{bmatrix}\bar{M} & \bar{S}_1 \\ \bar{S}_2 & \bar{I}\end{bmatrix}\begin{Bmatrix}\ddot{z}_s \\ \ddot{\theta}\end{Bmatrix} = \bar{q}S\left(\begin{Bmatrix}\bar{C}_{z_0} \\ \bar{C}_{m_0}\bar{c}\end{Bmatrix} + \begin{bmatrix}\bar{C}_{z_\alpha} & \bar{C}_{z_\delta} \\ \bar{C}_{m_\alpha}\bar{c} & \bar{C}_{m_\delta}\bar{c}\end{bmatrix}\begin{Bmatrix}\alpha_m \\ \delta\end{Bmatrix} + \begin{Bmatrix}\bar{C}_{z_q} \\ \bar{C}_{m_q}\bar{c}\end{Bmatrix}\frac{\dot{\theta}\bar{c}}{2V}\right) \quad (40)$$

where

$$\bar{M} = M - [C_{z_{\ddot{z}}}/g + C_{z_{\dot{\alpha}}}\bar{c}/2V^2 - C_{z_\alpha}(2\alpha_{m_{\ddot{z}}}V^2 + \alpha_{m_{\dot{\alpha}}}\bar{c}g)/2gV^2\alpha_{m_\alpha}]\bar{q}S \quad (41)$$

$$\bar{S}_1 = S_y - [C_{z_{\ddot{\theta}}}\bar{c}/2g - C_{z_{\dot{\alpha}}}\bar{c}\bar{x}/2V^2 - C_{z_\alpha}(\alpha_{m_{\ddot{\theta}}}V^2 - \alpha_{m_{\dot{\alpha}}}\bar{x}g)\bar{c}/2gV^2\alpha_{m_\alpha}]\bar{q}S \quad (42)$$

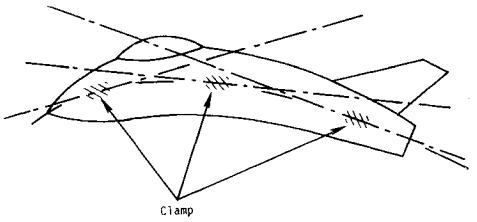

Fig. 1 Axes acceleration.

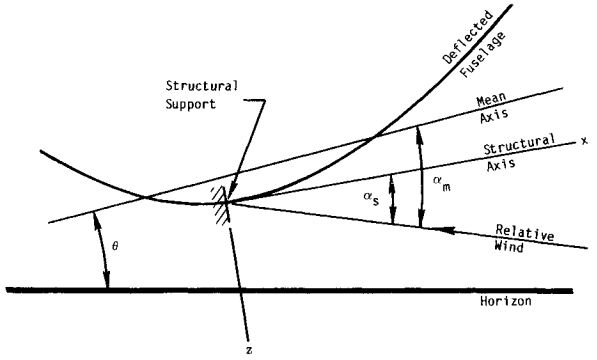

Fig. 2 Geometry of deformed flight vehicle.

$$\bar{S}_2 = S_y - [C_{m_{\ddot{z}}}/g + C_{m_{\dot{\alpha}}}\bar{c}/2V^2 - C_{m_\alpha}(2\alpha_{m_{\ddot{z}}}V^2 + \alpha_{m_{\dot{\alpha}}}\bar{c}g)/2gV^2\alpha_{m_\alpha}]\bar{q}S\bar{c} \quad (43)$$

$$\bar{I} = I_y - [C_{m_{\ddot{\theta}}}\bar{c}/2g - C_{m_{\dot{\alpha}}}\bar{c}\bar{x}/2V^2 - C_{m_\alpha}(\alpha_{m_{\ddot{\theta}}}V^2 - \alpha_{m_{\dot{\alpha}}}\bar{x}g)\bar{c}/2V^2\alpha_{m_\alpha}]\bar{q}S\bar{c} \quad (44)$$

$$\bar{C}_{z_0} = C_{z_0} - C_{z_\alpha}\alpha_{m_0}/\alpha_{m_\alpha} + (\Phi_{\tau_{\dot{\alpha}}} - C_{z_\alpha}\alpha_{m_{\dot{\alpha}}}/\alpha_{m_\alpha})\bar{c}g\cos\theta/2V^2 \quad (45)$$

$$\bar{C}_{m_0} = C_{m_0} - C_{m_\alpha}\alpha_{m_0}/\alpha_{m_\alpha} + (C_{m_{\dot{\alpha}}} - C_{m_\alpha}\alpha_{m_{\dot{\alpha}}}/\alpha_{m_\alpha})\bar{c}g\cos\theta/2V^2 \quad (46)$$

$$\bar{C}_{z_\alpha} = C_{z_\alpha}/\alpha_{m_\alpha} \quad (47)$$

$$\bar{C}_{m_\alpha} = C_{m_\alpha}/\alpha_{m_\alpha} \quad (48)$$

$$\bar{C}_{z_\delta} = C_{z_\delta} - C_{z_\alpha}\alpha_{m_\delta}/\alpha_{m_\alpha} \quad (49)$$

$$\bar{C}_{m_\delta} = C_{m_\delta} - C_{m_\alpha}\alpha_{m_\delta}/\alpha_{m_\alpha} \quad (50)$$

$$\bar{C}_{z_q} = C_{z_q} + C_{z_{\dot{\alpha}}} - C_{z_\alpha}(\alpha_{m_q} + \alpha_{m_{\dot{\alpha}}})/\alpha_{m_\alpha} \quad (51)$$

$$\bar{C}_{m_q} = C_{m_q} + C_{m_{\dot{\alpha}}} - C_{m_\alpha}(\alpha_{m_q} + \alpha_{m_{\dot{\alpha}}})/\alpha_{m_\alpha} \quad (52)$$

The solution of Eq. (40) is a routine problem in numerical integration. The Runge-Kutta method was used in the example problem after the equation was rewritten in state-variable form (the computer program utilized also has the capability of including autopilots). The initial conditions on α_m and δ are provided by the level flight trim solution, and the angle of attack is updated during the integration via

$$\alpha_m = (1/V)\int_0^t (\ddot{z}_s + V\dot{\theta} + g\cos\theta)\mathrm{d}\tau \quad (53)$$

An Example of a Forward-Swept-Wing Configuration

The example problem selected is a forward-swept-wing (FSW) configuration with a gross weight of 16,000 lb because of its importance in the current literature on static aeroelasticity. An extremely idealized configuration is shown in Fig. 3.

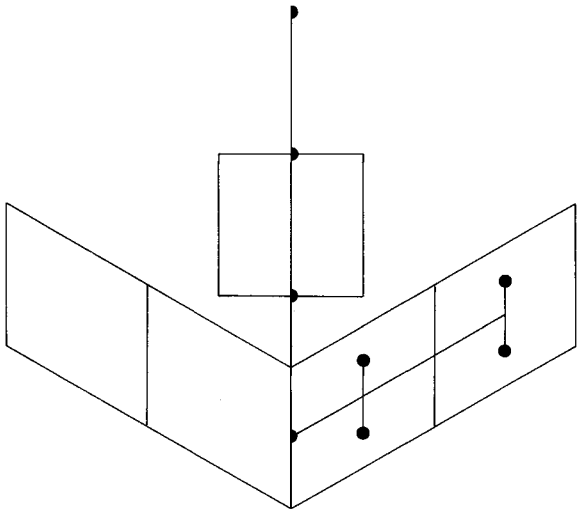

Fig. 3 Idealization of FSW configuration.

The wing has an aspect ratio of 4.0, no taper, no twist or camber, and a forward sweep angle of 30 deg; the canard has an aspect ratio of 1.0 and no taper, twist, camber, or sweep. The chords of the wing and canard are both 10.0 ft; the reference chord is chosen as $\bar{c}=10.0$ ft and the reference area is $S=400$ sq ft. The semispan of the wing is divided into two equal-width strips, as shown on the left wing in Fig. 3, for analysis by strip theory and the canard is analyzed as a single strip. Aerodynamic forces on the fuselage are neglected. In the subsonic strip theory for the wing and canard, a rigid chord is assumed¶ and the approximation for the the strip lift curve slope $c_{\ell_\alpha}=a_0\cos\Lambda$ is utilized where a_0 is the airfoil lift curve slope and Λ is the sweep angle; a_0 is taken as 5.0 per rad. The right wing in Fig. 3 shows the structural idealization. Four weights on each wing semispan are located along the centerlines of their respective strips and at the one-quarter and three-quarter chord locations, and are assumed to be connected to the 50% chord elastic axis by rigid streamwise bars. The weights are assumed to be 600 lb forward and 400 lb aft, giving a wing centroid at 45% of the wing chord. Each wing is assumed to be uniform with equal bending (EI_x) and torsion (GJ) stiffnesses of 25×10^7 lb-ft^2 and connected at its root to the fuselage. The fuselage is assumed to have the same bending stiffness as the wing and is shown with four equal and equidistant weights (1500 lb each per side); the fuselage length is 30.0 ft. The total weight per side is 8000 lb, the center of gravity is 12.82 ft forward of the intersection of the fuselage and wing elastic axis, and the centroidal moment of inertia in pitch per side is $I_{y_0}=892{,}900$ lb-ft^2.

Three structural support configurations are investigated to maximize the magnitudes of variations in the stability derivatives and response characteristics: one is a clamp at the forward end of the fuselage, the second is a clamp at the center of gravity (in order to assess Roskam's recommendation), and the third is a clamp at the intersection of the wing elastic axis and the fuselage centerline.

Vibration and flutter analyses have been performed on the example airplane to determine a speed regime for the maneuvering study in which the airplane is stable. The first three unrestrained frequencies are 9.886, 18.40, and 43.22 Hz. The modes are highly coupled and not readily described, although the first two appear to be primarily first wing bending and first fuselage bending, respectively. The flutter analysis utilized the British flutter method in NASTRAN,[18] assumed strip theory aerodynamics with the W.P. Jones approximation to the Theodorsen function (in order to avoid the singular effects of the Theodorsen function at low reduced frequency), and structural damping coefficients of $g=0.02$ in each mode. The flutter speed at sea level was found to be 1310 ft/s which corresponds to a dynamic pressure of $\bar{q}=2040$ psf. The flutter mode is a coupling between rigid body pitch and the first vibration mode; the flutter frequency is 4.48 Hz. This flutter mode is similar to that observed in the design studies of Miller, Wykes, and Brosnan.[19]

¶The assumption of only two chordwise control points on the lifting strips precludes accurate evaluation of the q-derivatives since the pitch rate is equivalent to a static parabolic camber deflection.[15]

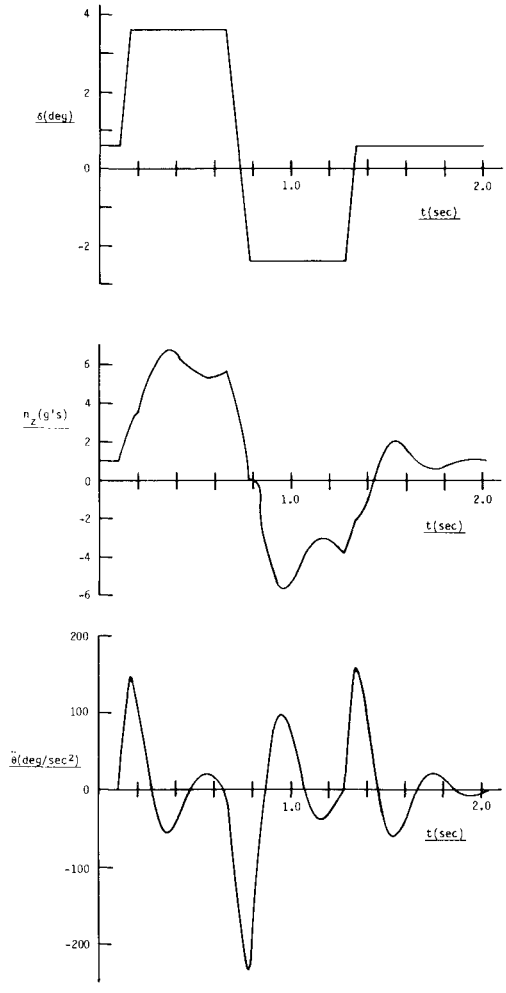

Fig. 4 Control input and maneuvering accelerations.

The example maneuver assumes a dynamic pressure of $\bar{q}=1200$ psf which corresponds to $V=1005$ ft/s and a Mach number of $M=0.90$ at sea level. Four sets of derivatives were determined for this flight condition: three sets were for the airplane restrained at the forward point, at the centroid, and at the aft point, and one set was for the unrestrained airplane calculated by the FLEXSTAB method. The $\dot{\alpha}$-derivatives were determined for the approximate short-period reduced frequency of $k=0.07$. Space does not permit tabulating these derivatives. The example control inputs are shown in Fig. 4. The airplane is in trimmed level flight for 0.10 s with an angle of attack $\alpha_m=0.128$ deg and canard position $\delta=0.611$ deg. Then a pullup is initiated and the control input rotates the canard at 50 deg/s to 3.611 deg at 0.16 s. At 0.66 s a pushover is begun and the canard position reaches -2.389 deg at 0.78 s. At 1.28 s the control is reversed and returns to the trim position at 1.34 s. The time histories of centroidal load factors and pitching accelerations using the four sets of stability derivatives and α_m-derivatives are found to be identical in five degree-of-freedom maneuvering analyses. The basic data were calculated with six significant figures and between five and six significant figures were found to agree among the

four sets of response accelerations. The common results from the four separate calculations are tabulated in the second column of Table 1 and are also presented graphically in Fig. 4.

We may now evaluate the consequences of disregarding the requirements for the mean axes, i.e., if we assume that $\alpha_m = \alpha_s$ in Eq. (36), as is implied in Refs. 7-9. In this case, all the α_m-derivatives vanish except for $\partial\alpha_m/\partial\alpha = 1.0$ in Eq. (37). The resulting incorrect solutions for the three different structural supports are tabulated in the last three columns of Table 1 and should be compared with the correct solution in the second column. In this example, the differences are not dramatic, and the assumption that $\alpha_m = \alpha_s$ is not an unreasonable approximation. However, in general, the magnitudes of the differences would be expected to be configuration dependent. The accuracy of the assumption $\alpha_m = \alpha_s$ could be a subject for further investigation on more practical configurations, but the present development should make the assumption no longer necessary.

The Speed Derivatives for Lift and Moment

Although the assumption of constant forward velocity has been made throughout the preceding development, the speed derivatives for lift and moment are readily found from the foregoing. The lift and moment coefficients at trim are functions of the incidence variables, accelerations ($\ddot{z} = g\cos\theta, \ddot{\theta} = 0$), Mach number, and dynamic pressure. If the trim airspeed V is perturbed by an amount v, the speed derivative is defined by

$$C_v = \left.\frac{\partial C(\alpha,\delta,\ddot{z},M,\bar{q})}{\partial(v/V)}\right|_{v=0} \tag{54a}$$

$$= V\frac{\partial C}{\partial M}\frac{\partial M}{\partial v} + V\frac{\partial C}{\partial \bar{q}}\frac{\partial \bar{q}}{\partial v} \tag{54b}$$

which becomes simply

$$C_v = M\frac{\partial C}{\partial M} + 2\bar{q}\frac{\partial C}{\partial \bar{q}} \tag{55}$$

At trim, the lift coefficient is

$$C_z = C_{z_0} + C_{z_\alpha}\alpha_s + C_{z_\delta}\delta + C_{z_{\ddot{z}}}\cos\theta \tag{56}$$

so the speed derivative for lift is

$$C_{z_v} = M\frac{\partial C_{z_0}}{\partial M} + 2\bar{q}\frac{\partial C_{z_0}}{\partial \bar{q}} + \alpha_s\left(M\frac{\partial C_{z_\alpha}}{\partial M} + 2\bar{q}\frac{\partial C_{z_\alpha}}{\partial \bar{q}}\right) + \delta\left(M\frac{\partial C_{z_\delta}}{\partial M} + 2\bar{q}\frac{\partial C_{z_\delta}}{\partial \bar{q}}\right) + \cos\theta\left(M\frac{\partial C_{z_{\ddot{z}}}}{\partial M} + 2\bar{q}\frac{\partial C_{z_{\ddot{z}}}}{\partial \bar{q}}\right) \tag{57}$$

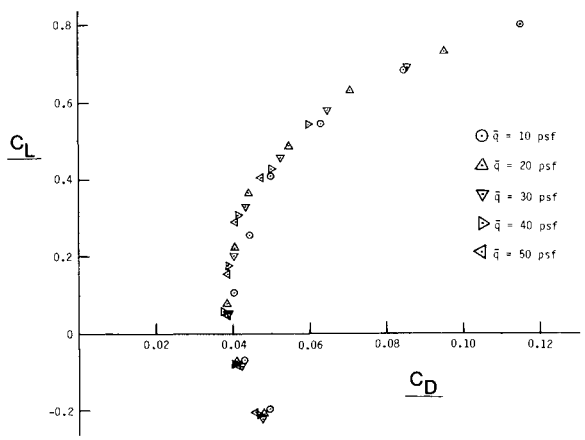

Fig. 5 Drag polar of flexible wing.

Table 1 Accelerations during maneuver for various SIC supports

Centroidal load factor, n_z(g's)

t(s)	Correct solutions: FLEXSTAB et al.	Incorrect solutions assuming $\alpha_m = \alpha_s$: Forward fixity	Centroidal fixity	Aft fixity
0.10	1.0	1.0	1.0	1.0
0.16	2.996	3.346	2.912	2.876
0.36	6.768	6.611	6.811	6.784
0.66	5.631	5.708	5.601	5.235
0.78	0.836	0.388	0.955	1.095
0.96	−5.619	−5.300	−5.706	−5.639
1.28	−3.726	−3.818	−3.682	−2.937
1.34	−1.987	−1.597	−2.071	−1.525
1.40	−0.916	−0.762	−0.972	−1.116
1.60	1.763	1.568	1.828	2.086
1.80	0.697	0.821	0.657	0.602
2.00	1.120	1.054	1.140	1.071

Pitching acceleration, $\ddot{\theta}$(deg/s^2)

t(s)	Correct solutions: FLEXSTAB et al.	Incorrect solutions assuming $\alpha_m = \alpha_s$: Forward fixity	Centroidal fixity	Aft fixity
0.10	0.0	0.0	0.0	0.0
0.16	144.0	127.1	148.0	149.8
0.36	−54.7	−46.2	−57.0	−58.8
0.66	4.3	0.6	5.8	25.7
0.78	−233.2	−212.5	−238.7	−246.5
0.96	99.0	82.0	103.8	106.4
1.28	1.3	5.4	−0.8	−39.9
1.34	157.6	138.1	161.9	135.6
1.40	93.2	86.6	95.7	105.1
1.60	−37.3	−27.5	−40.7	−56.9
1.80	14.9	8.5	17.0	22.3
2.00	−5.9	−2.5	−7.0	−4.9

The speed derivative for moment is given by a similar expression.

The derivatives with respect to M and $\bar{q}$ may be obtained numerically, as suggested by Kemp[9] by using the central difference formulas

$$\frac{\partial C}{\partial M} = \frac{C(M+\Delta M,\ \bar{q}) - C(M-\Delta M,\bar{q})}{2\Delta M} \tag{58}$$

$$\frac{\partial C}{\partial \bar{q}} = \frac{C(M,\bar{q}+\Delta\bar{q}) - C(M,\bar{q}-\Delta\bar{q})}{2\Delta\bar{q}} \tag{59}$$

The small perturbations ΔM and $\Delta\bar{q}$ must be large enough that the close differences do not lose significance.

Concluding Remarks

The correct formulation of the equations of motion of an elastic flight vehicle has been presented for the case in which the structural flexibility is given in terms of a flexibility matrix of the vehicle restrained in a statically determinate manner. The relationship that has been missing in previous analyses of the problem has been established in the rotations of the mean axes relative to the structural axes as caused by each aerodynamic and inertial loading. The modified form of the equations of motion that results from inclusion of the mean axis rotations has been presented, and the correctness of the formulation has been demonstrated by identical numerical results from four case studies of longitudinal maneuvering of an example forward-swept-wing airplane using the mean axis formulation (FLEXSTAB) and three significantly different

structural axis formulations. The errors consequent to disregarding the requirements for the mean axes have been evaluated on the example airplane for the three different structural axes, but it is noted that the errors would be configuration dependent.

The longitudinal equation of motion has not been mentioned since it was secondary to our basic concerns, although aeroelastic speed derivatives have been discussed briefly. Aeroelastic effects on drag are another matter. It is commonly assumed[7,8,20,21] that these are negligible. This is not entirely the case. Aeroelastic effects seem to have a negligible effect only on the drag polar of the individual *components* of an airplane but not for the entire vehicle *trimmed* drag polar, as has been shown by an elementary analysis in Ref. 22. A drag polar measured[23] on a low-speed aeroelastic (flutter) model of the Douglas XA3D-1 airplane is presented in Fig. 5 for an intermediate horizontal tail setting ($i_t = 1$ deg; settings of $i_t = -2$ deg, $+4$ deg and tail-off were also measured). Since only the wing was flexible on the model, the data of Fig. 5 support the conclusion of Ref. 22 that the *component* drag polar is not affected by flexibility. However, the trim drag requires further investigation. A theoretical investigation would require an accurate aerodynamic method for estimating induced drag on flexible surfaces, such as the subsonic quasivortex lattice method of Lan.[24]

This analysis has assumed quasisteady structural equilibrium during maneuvering. However, if the controls are moved abruptly, dynamic structural effects and aerodynamic lags may be significant. Dynamic structural effects can be added to the formulation by the mode acceleration method for transient response and aerodynamic lags can be added by the Padé approximant method of representing transient aerodynamic loading. The addition of dynamic structural effects to the longitudinal equation of motion would also result in small aerodynamic propulsion terms that could be obtained, e.g., from the unsteady version of Lan's method.[25]

Acknowledgments

The authors wish to thank Dr. Malcolm J. Abzug of ACA, Inc., for stimulating discussions and helpful suggestions during the preparation of this paper, They would also like to express their appreciation to him for his computation of the time histories presented using his FLY4 six degree-of-freedom maneuvering analysis, modified to account for the mean axis rotations of the flexible vehicle.

The authors also wish to thank E. Dean Bellinger of The MacNeal-Schwendler Corp., for obtaining the flexibility matrices for the three support conditions and performing the flutter analysis of the example configuration using MSC/NASTRAN.

References

[1]Bisplinghoff, R. L. and Ashley, H., *Principles of Aeroelasticity,* John Wiley and Sons, New York, 1962; reprinted by Dover Publications, New York, 1975

[2]Milne, R. D., "Dynamics of the Deformable Aeroplane," British Aeronautical Research Council, R&M 3345, 1964.

[3]Milne, R. D., "Some Remarks on the Dynamics of Deformable Bodies," *AIAA Journal,* Vol. 6, March 1968, pp. 556-558.

[4]Anon., "An Analysis of Methods for Predicting the Stability Characteristics of an Elastic Airplane—Summary Report," NASA CR-73277, Nov. 1968.

[5]Dusto, A. R., et al., "A Method for Predicting the Stability Derivatives of an Elastic Airplane; Vol. I-FLEXSTAB Theoretical Description," NASA CR-114712, Oct. 1974, see also AFFDL TR-74-91, Vol. 1, Nov. 1974, pp. 4-4 to 4-26, 5-11 to 5-14.

[6]Wykes, J. H., and Lawrence, R. E., "Aerothermoelasticity: Its Impact on Stability and Control of Winged Aerospace Vehicles," *Journal of Aircraft,* Vol. 2, Nov.-Dec. 1965, pp. 517-526.

[7]Roskam, J., *Flight Dynamics of Rigid and Elastic Airplanes,* Roskam Aviation and Engineering Corp., Lawrence, Kansas, 1972.

[8]Roskam, J., *Airplane Flight Dynamics and Automatic Flight Controls,* Roskam Aviation and Engineering Corp., Lawrence, Kansas, 1979.

[9]Kemp, W. B., Jr., "Definition and Application of Longitudinal Stability Derivatives for Elastic Airplanes," NASA TN D-6629, 1972.

[10]Rowan, J. C., and Burns, T. A., "Aeroelastic Loads Predictions Using Finite Element Aerodynamics," *Journal of Aircraft,* Vol. 12, Nov. 1975, pp. 890-898.

[11]Bisplinghoff, R. L., Ashley, H., and Halfman, R. L., *Aeroelasticity,* Addison-Wesley Publishing Co., Reading, MA, 1955, p. 449.

[12]Rodden, W. P. and Revell, J. D., "The Status of Unsteady Aerodynamic Influence Coefficients," Institute of the Aeronautical Sciences, New York, Fairchild Publication Fund Paper No. FF-33, Jan. 1962.

[13]Giesing, J. P., Kalman, T. P., and Rodden, W. P., "Correction Factor Techniques for Improving Aerodynamic Prediction Methods," NASA CR-144967, May 1976.

[14]Rodden, W. P., "On Vibration and Flutter Analysis with Free-Free Boundary Conditions," *Journal of the Aeronautical Sciences,* Vol. 28, Jan. 1961, pp. 65-66.

[15]Rodden, W. P., and Giesing, J. P., "Application of Oscillatory Aerodynamic Theory to Estimation of Dynamic Stability Derivatives," *Journal of Aircraft,* Vol. 7, May-June 1970, pp. 272-275, see also Errata and Addenda *Journal of Aircraft,* Vol. 21, Jan. 1984, pp. 92-94.

[16]Rodden, W. P., "Errata, 'Aeroelastic Divergence of Unrestrained Vehicles'," *Journal of Aircraft,* Vol. 21, Jan. 1984, pp. 94-96.

[17]Letsinger, G. R., "Effect of Aeroelasticity on Airplane Stability and Control with Special Reference to an Application of FLEXSTAB to the F-111 TACT I Airplane," Symposium on Transonic Aircraft Technology, Technical Report AFFDL-TR-78-100, Aug. 1978

[18]Rodden, W. P., Harder, R. L., and Bellinger, E.D., "Aeroelastic Addition to NASTRAN," NASA CR 3094, March 1979.

[19]Miller, G. D., Wykes, J. H., and Brosnan, M. J., "Rigid-Body Structural Mode Coupling on a Forward Swept Wing Aircraft," *Journal of Aircraft,* Vol. 20, Aug. 1983, pp. 696-702.

[20]Etkin, B., *The Dynamics of Atmospheric Flight,* John Wiley & Sons, New York, 1972.

[21]Seckel, E., *Stability and Control of Airplanes and Helicopters,* Academic Press, New York, 1964.

[22]Rodden, W. P., Surber, T. E., and Vetter, H. C., "The Effect of Flexibility on the Drag Polar of an Aircraft." *Journal of the Aeronautical Sciences,* Vol. 24, June 1957, pp. 456-458.

[23]Ogawa, H., "Report of Wind-Tunnel Tests on a 1/12 Scale Aeroelastic Model of the Douglas (El Segundo) XA3D-1 Airplane," GALCIT Rept. 601, California Institute of Technology, Pasadena, CA, April 30, 1953.

[24]Lan, C. E., "A Quasi-Vortex-Lattice Method in Thin Wing Theory," *Journal of Aircraft,* Vol. 11, Sept. 1974, pp. 518-527.

[25]Lan, C. E., "The Unsteady Quasi-Vortex-Lattice Method with Applications to Animal Propulsion," *Journal of Fluid Mechanics,* Vol. 93, Part 4, 1979, pp. 747-765.